

Investigations of reticulated porous alumina foam ceramics based on different coating techniques with the aid of μ CT and statistical characteristics

Claudia Voigt^{a,*}, Eva Jäckel^b, Christos G. Aneziris^a, Jana Hubálková^a

^aTechnical University Bergakademie Freiberg, Department of Ceramics, Glass and Construction Materials Technology, Agricolastr. 17, 09599 Freiberg, Germany

^bTechnical University Bergakademie Freiberg, Institute of Foundry Technology, Bernhard-von-Cotta-Straße 4, 09599 Freiberg, Germany

Received 13 July 2012; received in revised form 31 August 2012; accepted 1 September 2012

Available online 11 September 2012

Abstract

Alumina foam ceramic filters were prepared due to the “replica technique”. The parameters of the two coating steps were varied to find the optimal processing route to prepare ceramic foam filters with a good homogeneous distribution of the strut thickness. Different additives for the slurry for the impregnation (first coating) step were investigated with the aid of rheological measurements. For the second coating step spraying as well as centrifuging techniques with different processing parameters were studied. The sintered foam structure (strut diameter, pore size and porosity) was characterized with the aid of CT-images and described with an image analysis software and statistical tools.

The mechanical properties depend strongly on the achieved structure of the filter and especially on the distribution of the strut thickness in the inner volume side of the filter. A centrifuging technique with a pressure supported dipping as well as optimum processing parameters of the spraying step led to improved mechanical properties as well as homogenous macro-structures.

© 2012 Elsevier Ltd and Techna Group S.r.l. All rights reserved.

Keywords: Alumina; Rheology; Homogeneity; Reticulated porous ceramics

1. Introduction

Since the 70s ceramic foam filters are used for the filtration of molten metal. The filters generate a laminar flow of the liquid metal and prevent so the formation of new inclusions. Secondly, they remove non-metallic inclusions, whereby the dominant filtration mechanism for small particles is the so called deep bed filtration [1]. Foam ceramic filters based on silicon carbide and alumina are widely used for the filtration in aluminum foundries. Investigations within the frame of the Collaborative Research Center 920—“Multi-Functional Filters for Metal Melt Filtration”, granted by the German Research Foundation (DFG), aims to improve mechanical properties of casted metallic materials with the aid of functionalized filter surfaces, whereby the alumina foam filters

are used as a reference pattern. Furthermore it will be utilized as a skeleton for the different coatings.

The “replica process” by Schwartzwalder is an established processing route for preparation of ceramic foam filters [2]. This process uses polymeric foam which is coated with a ceramic slurry. After drying the polymer is burned out and the ceramic material is sintered, whereby a replica of the original polymeric foam is produced. In most cases two coating steps are required. In the first coating step the polymeric foam is immersed into the slurry, followed by removing the excess slurry with a set of rollers or a centrifuge [3]. A second coating step follows after a drying step based on spraying at room temperature [4] or centrifuging [3]. This second step eliminates defects which are formed during the first coating. In addition the critical strut thickness can be adjusted [5]. For both coating steps, the rheological behavior of the ceramic slurry plays a key role; the ceramic slurry must possess a shear-thinning behavior [6,7]. Besides the slurry has

*Corresponding author.

E-mail address: claudia.voigt@ikgb.tu-freiberg.de (C. Voigt).

to be fluid enough to enter the polymeric foam but the viscosity has to be high enough to remain in the foam after treatment [8].

In the first part of this paper, the contribution of different processing additives for a homogenous first coating step will be investigated. In the second part, different processing techniques and their impact on mechanical properties of ceramic filters and homogeneity of the macro-structure will be explored.

2. Materials and methods

Commercial polyurethane foams with 20 ppi (pores per inch) and a size of 50 mm × 50 mm × 22 mm were used for the experiments. The slurries consist of three different alumina powders provided by Almatix (33 wt% tabular alumina, T60/64 0–0.045 mm, 33 wt% calcined alumina CT 9 FG, $d_{50}=5\text{ }\mu\text{m}$, and reactive alumina 33 wt% CT 3000 SG, $d_{50}=0.5\text{ }\mu\text{m}$), deionised water and processing additives based on Optapix AC 170 (Zschimmer & Schwarz, Germany); Dolapix CE 64 (Zschimmer & Schwarz, Germany); Axilat RH 50 MD (C.H. Erbslöh, Germany); polypropylene glycol P400 (Aldrich Chemistry, USA).

Axilat RH 50 MD is a xanthan acting as thickening agent. Optapix AC 170 acts as a binder and is an aqueous dispersion of polymers. Dolapix CE 64 (carboxylic acid preparation) contributes as a dispersant and polypropylene glycol P400 is used as a wetting agent. The slurries were prepared in a ToniMIX high shear mixer (Tonitechnik, Germany). At the beginning the dry components were mixed, followed by the addition of the additives in the order Optapix, Dolapix and PPG 400. By adding a part of the water a plastic mass is formed and kneaded for 5 min in order to destroy the agglomerates. While continuing the stirring, the rest of the deionised water is added. The ToniMIX is suitable for high viscous slurries but for mixtures with low viscosities separations of the mixture are observed. Therefore a second mixing step with a RZR 2102 control (Heidolph, Germany) was applied to reach a higher homogeneity of the slurry.

The rheological behavior of the different slurries was measured with the aid of a rheometer RheoStress RS 150 (Haake, Germany). The slurries for the first coating step were measured with the coaxial cylinder measuring system of the type Z10 DIN, for the second coating slurries the Z40 DIN was used. The rheological behavior was explored by measuring the shear stress as a function of the shear rate. The measurement of the shear stress starts after a relaxing time of 20 s when the shear rate increases in 300 s to 1000 1/s. After a holding time of 90 s at 1000 1/s, it decreases within 300 s to zero. With the help of the measured shear stress the viscosity was calculated. The Yield stress was measured by increasing the shear stress between 0.01 and 80 Pa in 300 s. The thixotropy and the yield stress were determined from the rheological measurement with the help of the program RheoWin Data Manager (Haake, Germany).

2.1. The first coating step

For the first coating step the polyurethane foams were immersed in the slurry and then passed two times through rotating rollers with a distance of 20% of the height of the ceramic foam [7] to remove the excess slurry. After the first coating the foam ceramics were dried and weighed. To determine the applied mass, the mass of the polyurethane foam was subtracted from the weighed mass of the dried not sintered ceramic samples.

In order to investigate the impact of the additives on the applied mass, the viscosity and the thixotropy, different compositions with only one variable were prepared, see Table 1. The solid content was held uniform for the variation of Optapix AC 170, Dolapix CE 64 and polypropylene glycol P400. Since Axilat RH 50 MD itself strongly absorbs water, the solid content of the compositions with variable Axilat RH 50 MD concentration should be varied as well. The highest solid content for every Axilat concentration was chosen as the lowest processable water amount.

2.2. The second coating step

For the investigation of the second coating step, a slurry composition with different solid contents was used (0.5 wt% Axilat, 1 wt% Optapix AC 170, 0.6 wt% Dolapix CE 64, 0.84 wt% polypropylene glycol P400 and solid contents of 71.4 wt% and 76.9 wt%), (Table 2). Two different coating methods were applied: spraying and centrifugation. For spraying a spray gun SATAjet B (Sata, Germany) with a nozzle diameter of 1.4 mm and a spraying pressure of 3 bar was used. Hasterok et al. [4] used a distance between nozzle and filter of 27 cm and an additional airstream to reach a better transport of the slurry into the foam. Both parameters were tested in the present work. Furthermore a distance between nozzle and foam of 5 cm was used to analyze the influence of the airstream velocity. Table 2 gives an overview over the applied parameters.

The centrifugation was performed using a Megafuge 1.0 (Heraeus, Germany). The polyurethane foams with the first coating were dipped into the slurry and then the centrifugation process followed to remove the excess slurry. For a good homogeneity of the coating layer it is essential to reach a complete filling of the foam while dipping into the slurry. For slurries with a high viscosity, the application of pressure onto the slurry while dipping was tested. The solid content was also varied. After drying of the second coating, the foams were burned out at 600 °C [9] with a heating rate of 1 K/min and a holding time of one hour, and then sintered at 1600 °C with a heating rate of 2 K/min and a holding time of one hour.

During the preparation special attention was paid to reach the same weight after the second coating for all variations of the ceramic foams. On the assumption that the ceramic foams are homogenous and have the same weight, the strut diameter distribution should be uniform.

Table 1

Compositions and results of the investigated slurries for the first coating (for determining the applied mass at least 10 samples for each variation were tested).

No	Solid content (wt%)	Axilat RH 50 MD (wt%)	Optapix AC 170 (wt%)	Dolapix CE 64 (wt%)	PPG 400 (wt%)	Applied mass (g)	Viscosity at 214 s ⁻¹ (Pa s)	Thixotropy (kPa/s)
1	90.9	0.1	1	0.6	0.84	26.6 ± 1.5	31.2	2483
2	89					15.3 ± 0.6	5.2	724
3	87					15.1 ± 0.7	1.1	83
4	85.1					12.5 ± 0.6	0.3	3
5	87	0.3				15.4 ± 0.4	7.6	776
6	85.1					14.1 ± 0.5	3.7	347
7	83.3					13.2 ± 0.4	2.2	192
8	83.3	0.5				15 ± 0.7	2.5	166
9	81.6					13.1 ± 0.6	2.5	176
10	80					12 ± 0.6	1.8	105
11	80	0.7				12 ± 0.5	2.1	166
12	78.4					11.7 ± 0.6	2	65
13	76.9					11.3 ± 0.6	1.6	39
14	83.3	0.5	0.7	0.6	0.84	16.6 ± 0.6	4.4	433
15			1			15.7 ± 0.7	4.9	419
16			1.3			16.2 ± 0.5	4	258
17	83.3	0.5	1	0.3	0.84	15.6 ± 0.6	2.9	514
18				0.6		15.5 ± 0.5	3.1	222
19				0.9		15.4 ± 0.6	3.9	280
20	83.3	0.5	1	0.6	0.5	15.3 ± 0.8	3.8	204
21					0.84	15.7 ± 0.8	3.2	419
22					1	15.2 ± 0.5	3.4	252

Table 2

Overview of the tests for the second coating.

No	Solid content (wt%)	Method	Remarks	Mean weight of the filters (g)
A	76.9	Centrifuge	With pressure	31.6 ± 1.8
B			Without pressure	27.4 ± 1.4
C		Spray	Distance 5 cm	27.8 ± 1.6
D			Distance 27 cm	27.3 ± 0.6
E			Distance 27 cm with additional air flow	28.1 ± 1.2
F	71.4	Centrifuge	With pressure	32.1 ± 1.2
G			Without pressure	28.8 ± 1.1
H		Spray	Distance 5 cm	28.8 ± 1.1
I			Distance 27 cm	27.6 ± 1.8
J			Distance 27 cm with additional air flow	28.1 ± 0.6

Only then differences in the results can be attributed to an inhomogeneity of the coating application.

2.3. Characterization of the filters

The compression strength of the ceramic foams was measured with a Tiratest 2420 (TIRA GmbH, Germany) with the loading rate of 20 mm/min. In order to apply stress on the weakest link of the ceramic foam structure two bearings with a diameter of 25 mm were used. The homogeneity of the ceramic foam structure was evaluated with the aid of a micro focus X-ray computer tomograph CT-ALPHA (ProCon X-Ray,

Germany) equipped with a 160 kV X-ray tube and a Hamamatsu detector (79425 K-05) with 2400 × 2400 active pixels. The reconstructed CT data were analyzed with the software Modular Algorithms for Volume Images (MAVI, Fraunhofer, Germany) with regard to the sizes of the pores, the amount of porosity and the diameter of the struts. The reconstructed 3D data should first be processed. The different processing steps used in this study are presented in Fig. 1 and Table 3.

A “Small Impingement Test” was carried out to test the thermal shock behavior of the filters. The test equipment consists of a sodium silicate bonded pouring basin on the top of a metal frame. The filter is fixed at the bottom of pouring

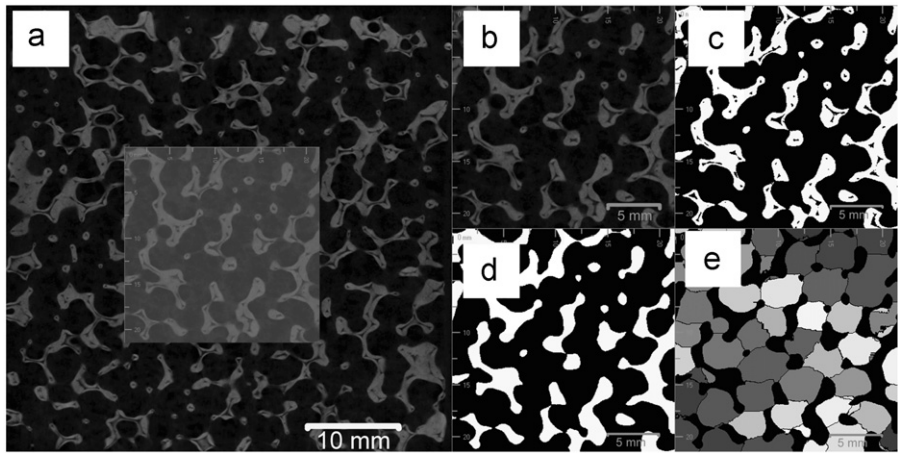


Fig. 1. Image processing steps using MAVI (a) reconstructed CT data, (b) cropped inner part of the filter, (c) binarisation with Otsu threshold, (d) filter structure with closed voids and (e) applying the feature “complex morphology”.

Table 3
Processing steps in MAVI for determining the porosity, the pore size and the strut diameter.

Porosity	Pore diameter	Strut diameter
Cropping the edges, see Fig. 1b		
Binarisation (with Otsu’s Threshold), see Fig. 1c		
Field features	Steps for closing the porosity created by the PU sponge	
	1) Closing step with cube with a size of 5	
	2) Labeling with neighborhood 6/4 for removing the rest of the PU pores	
	3) Binarisation, see Fig. 1d	
	Determining the macro pore size with the feature complex morphology and object feature, see Fig. 1e	Determining the diameter of the edges with open foam features (with the model Laguerre force biased CV=0.2 and euler number density based)

basin with common core adhesive. Each filter is thermal and mechanical stressed with 3 kg molten aluminum alloy with 7 wt% Si and 0.3 wt% Mg referring to European standard EN AC—AlSi7Mg0.3. The drop height of the liquid aluminum was around 30 cm. The pouring temperature was set at 750 °C, which is slightly higher than the common pouring temperature. The filter passes the test when it does not break during the casting.

3. Results

3.1. The first coating step

According to Yao et al. [6] and Studart et al. [7] the slurry should have a shear-thinning behavior. The rheological requirement was fulfilled for all tested 22 slurries. Fig. 2 shows the shear stress and the dynamic viscosity as a function of the shear rate of the slurry no. 5 (0.3 wt% Axilat RH 50 MD and 87 wt% solid content) as a representative for the tested slurries. For the slurries with varied amount of Axilat RH 50 MD and solid content there are significant differences in the applied mass, viscosity and thixotropy, (Fig. 3 and Table 1). Following mixtures show a poor coating behavior,

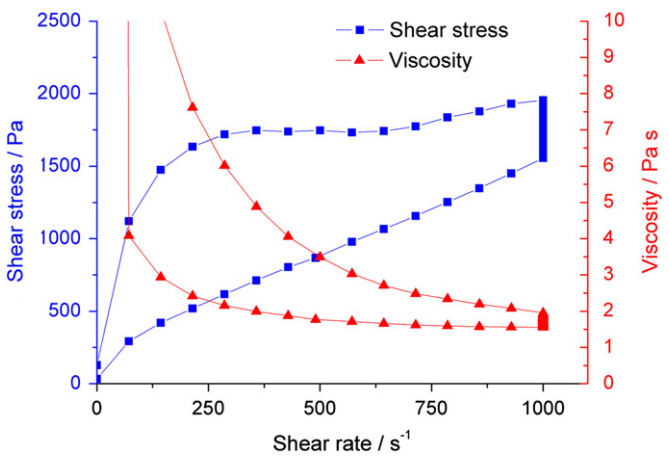


Fig. 2. Rheological behavior of a first coating slurry no. 5 (0.3 wt% Axilat, 87 wt% solid content—measured with the coaxial cylinder measuring system of the type Z10 DIN).

slurry no. 1, 3 and 4 (0.1 wt% Axilat with 90.9 wt%, 87 wt% and 85.1 wt% solid content). Slurry no. 1 had a high viscosity and thixotropy and, therefore it was not possible to remove the excess slurry with the rollers. Due to its low viscosity, the slurries no. 3 and 4 did not remain at the polyurethane struts;

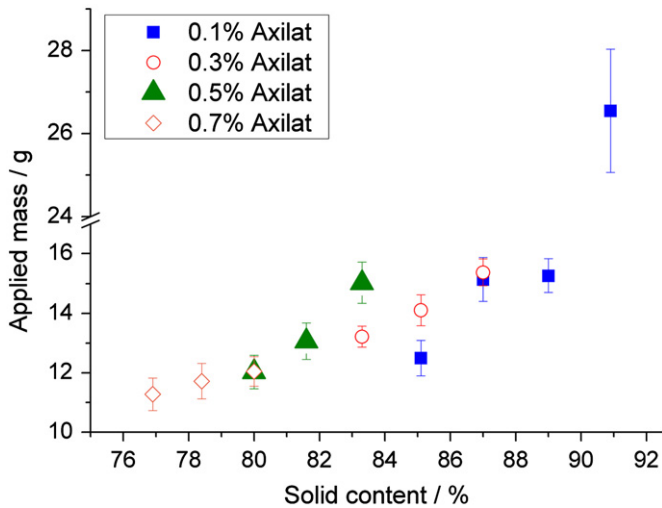


Fig. 3. Applied mass in dependence on the solid content and the concentration of the thickening agent Axilat RH 50 MD.

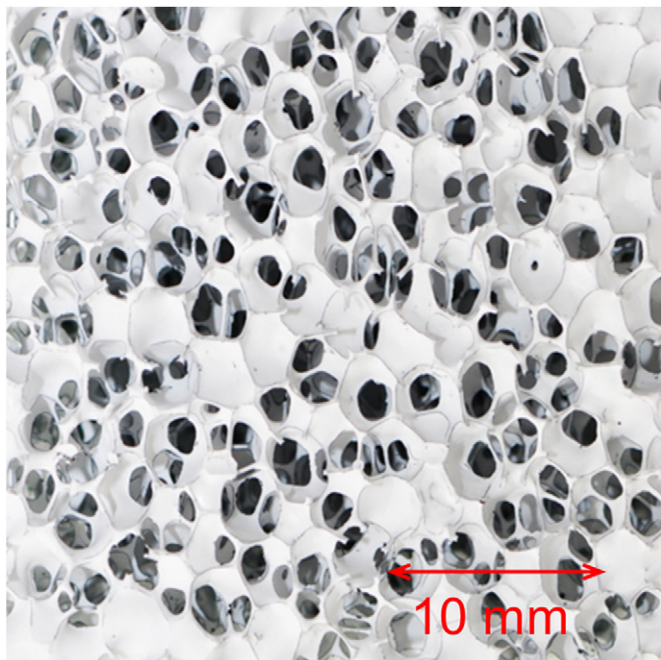


Fig. 4. Photograph of an unsintered polyurethane foam with first coating slurry no. 4 (85.1 wt% solid content, 0.1 wt% Axilat).

they dropped from the top to the bottom of the foam and so an inhomogeneous coating was formed, Fig. 4. Fig. 5 shows a polyurethane foam with a good ceramic coating which was achieved with the slurries 2, 5–22. The results demonstrate that the thickening agent Axilat is needed to provide slurry with optimal rheological properties for the coating. There is an optimum concentration between 0.3 wt% and 0.5 wt% Axilat. A higher concentration is linked with a higher water demand and so with a decrease in the applied mass. Slurries with a lower concentration of Axilat (0.1 wt% Axilat) show a strong sensitivity to the solid content which is not recommended for impregnating slurry. Comparing the 9 slurries (variation of the Axilat RH 50 MD) with a good coating

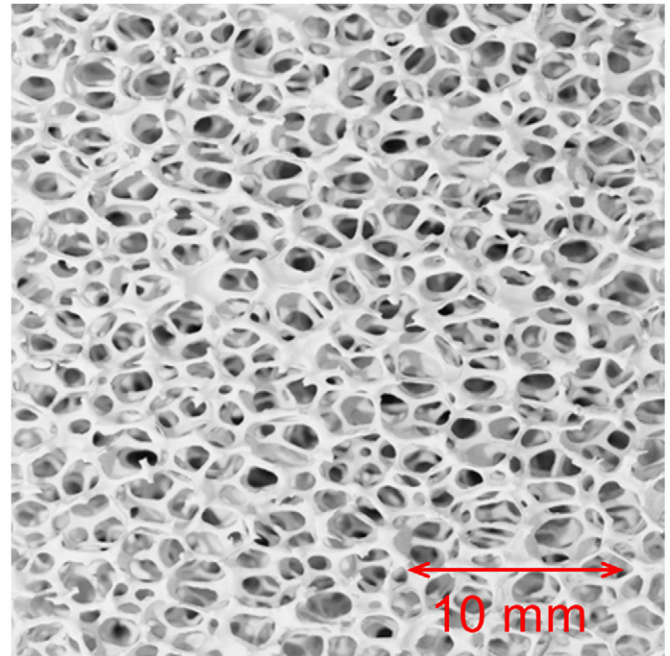


Fig. 5. Photograph of an unsintered polyurethane foam with first coating slurry no. 5 (87 wt% solid content, 0.3 wt% Axilat).

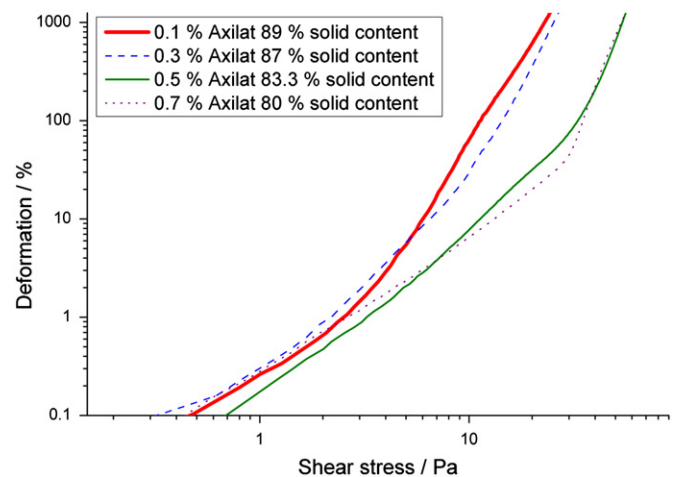


Fig. 6. Yield stress of slurries with different concentrations of the thickening agent (Axilat RH 50 MD) and solid content.

performance of Fig. 3 shows clearly that with decreasing solid content decreases the applied mass. Fig. 6 shows four characteristic yield stress measurements of slurries as a function of different Axilat concentrations. Higher yield stresses are achieved by increasing Axilat and solid content.

The variation of the Optapix AC 170, the Dolapix CE 64 and the polypropylene glycol P400 (in the chosen limits) has no significant influence on the coating results (Table 1).

3.2. The second coating step

Both slurries tested for the second coating step possess a shear-thinning behavior with a thixotropic loop, see Fig. 7. The investigated coating processes (centrifugation and

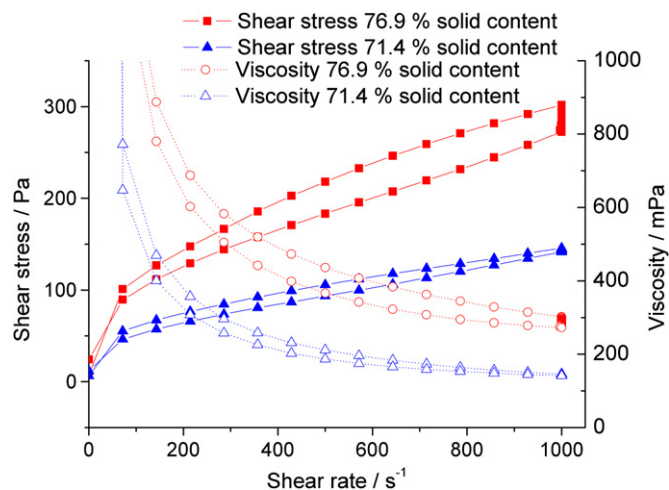


Fig. 7. Rheological behavior of the two second coating slurries with the slurry composition 0.5 wt% Axilat, 1 wt% Optapix AC 170, 0.6 wt% Dolapix CE 64, 0.84 wt% polypropylene glycol P400 and solid content of 71.4 wt% and 76.9 wt%—measured with the coaxial cylinder measuring system of the type Z40 DIN).

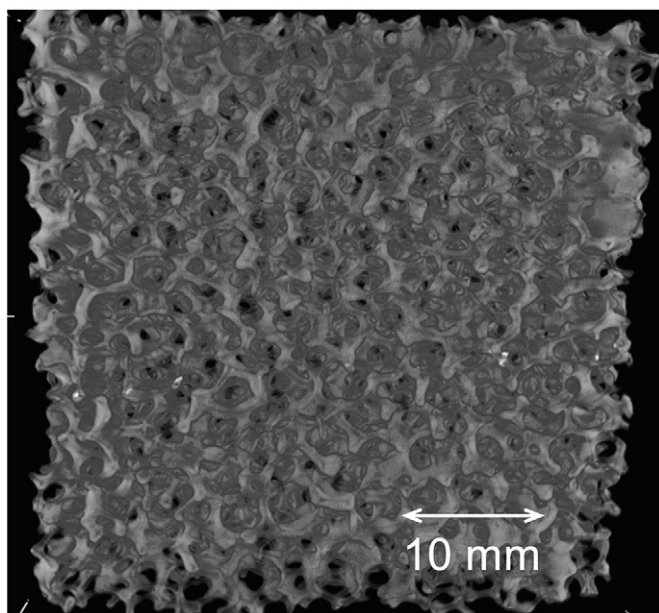


Fig. 8. Volume rendering of a ceramic foam filter.

spraying) and the varied parameters have a great influence on the quality of the produced ceramic foams.

The ceramic foams prepared by the spraying process with a distance of 27 cm have narrowed pores at the surface. Centrifuged samples possess more open pores.

In Fig. 8 the volume rendering of a ceramic foam filter (centrifuged with pressure and 71.4 wt% solid content is demonstrated). The mathematical description of the reconstructed volume data sets was carried out by means of MAVI [11]. In order to avoid a falsification through edge effects only the inner part of the ceramic foam was analyzed by MAVI. So the data processing started with a cropping step, see Fig. 1 and Table 3. This step was followed by binarisation with Otsu's threshold. The binarised images were

Table 4

MAVI results and compression strength of the different variations of the coating step 2 (mean value of the filter) (for determining the compression strength at least 8 samples for each variation were tested).

	Compression strength (MPa)	Mean porosity (%)	Mean strut diameter (mm)	Mean pore size (mm)
<i>71.4 wt% solid content</i>				
Centrifuge + pressure	2.91 ± 0.68	75.9	0.67	4.07 ± 1.51
Centrifuge	2.43 ± 0.43	80.6	0.63	4.19 ± 1.45
Spray 5 cm	2.07 ± 0.52	79.9	0.65	4.28 ± 1.48
Spray 27 cm	1.16 ± 0.21	83.6	0.59	4.25 ± 1.45
Spray 27 cm with air stream	1.00 ± 0.26	81.1	0.67	3.97 ± 1.52
<i>76.9 wt% solid content</i>				
Centrifuge + pressure	2.73 ± 0.51	77.2	0.66	4.06 ± 1.46
Centrifuge	1.78 ± 0.46	81.7	0.63	4.20 ± 1.43
Spray 5 cm	1.54 ± 0.41	83.0	0.66	3.99 ± 0.62
Spray 27 cm	1.00 ± 0.13	83.5	0.61	4.10 ± 0.60
Spray 27 cm with air stream	0.77 ± 0.37	84.7	0.61	4.38 ± 1.48

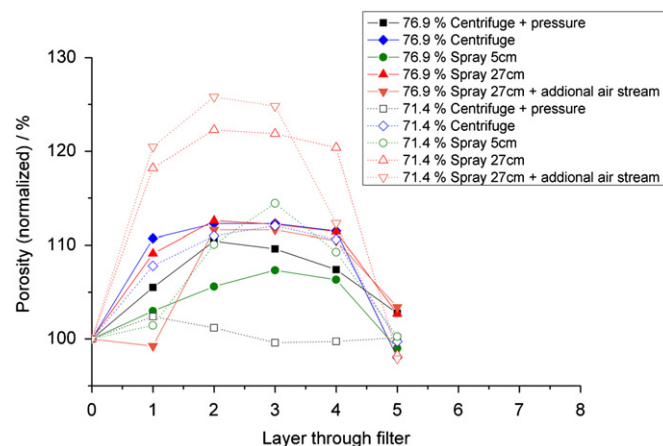


Fig. 9. Normalized porosity in dependence on the position in the foam.

used to analyze the porosity of the filters applying the “field feature” procedure. In order to identify the structural components of the filter (pores and struts) a segmentation step was necessary. Due to the fact, that the polyurethane foams generate voids after debinding (sharp edged pores inside the struts and nodes) morphological operations “closing” and “labeling” were applied to remove these voids and analyze so the real -for the filtering mechanism crucial- macro porosity. Afterwards, the macro pores size were determined by the feature “complex morphology” and “object features”. Supplementary, the diameters of the struts were calculated by “open foam features”.

The mean values of each variation are listed in Table 4. In the next step every filter was cut into six layers (along the height of the sample) to verify the homogeneity of the sample in dependence on the position in the foam, see Figs. 9 and 10. For every variation the maximum difference between the six layers was calculated (for the porosity and the strut diameter) and plotted in Fig. 11. The diagram shows that the samples centrifuged with pressure

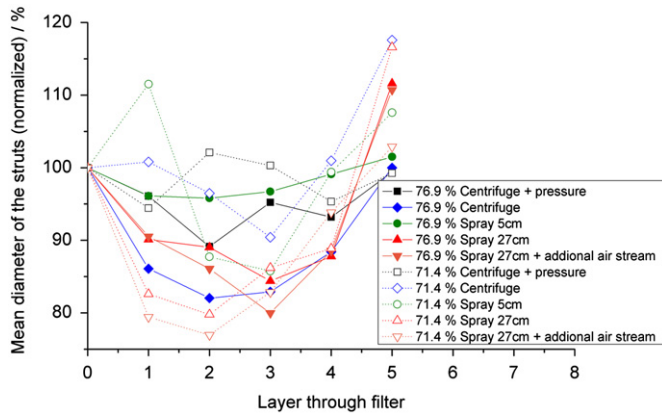


Fig. 10. Normalized mean strut diameter in dependence on the position in the foam.

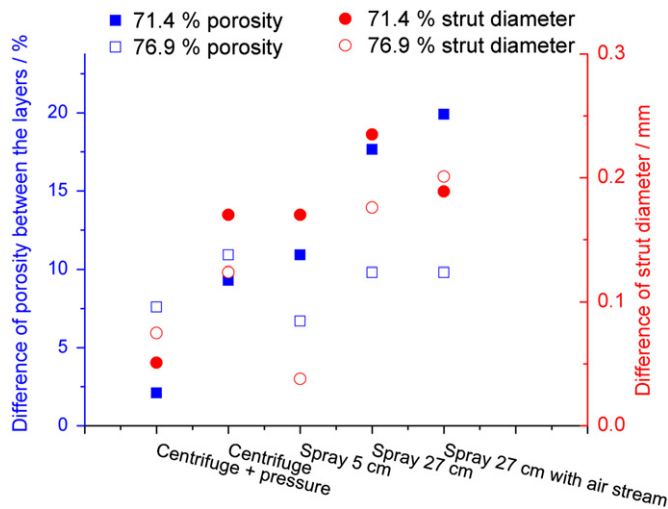


Fig. 11. Maximum difference of the porosity and strut diameter of the different layers.

(71.4 wt% and 76.9 wt% solid content) and the sprayed sample with a distance of 5 cm and a solid content in the range of 77 wt% possess the lowest differences and so the highest homogeneity. Contrary to Hasterok et al. [4] the largest scattering of the porosity and the strut thickness values was observed for the samples which were sprayed with a distance of 27 cm (with and without additional air stream). The different composition of the slurries – zirconia slurries instead of alumina slurries – and the smaller pore size of the polyurethane foam (Hasterok et al. used 30 ppi) are assumed to be the main sources for the different results. According to Fig. 9, for spraying the higher solid content and for centrifuging the lower solid content should be preferred.

These scattering of the values between the different variations are confirmed by the results of the compression strength tests, (Fig. 12). The smallest values of the mean compression strength (around 1 MPa) were measured for the sprayed filters with a distance of 27 cm. There is no significant difference between the two different solid contents and between with and without additional air stream. The spraying process with a distance of 5 cm offers better

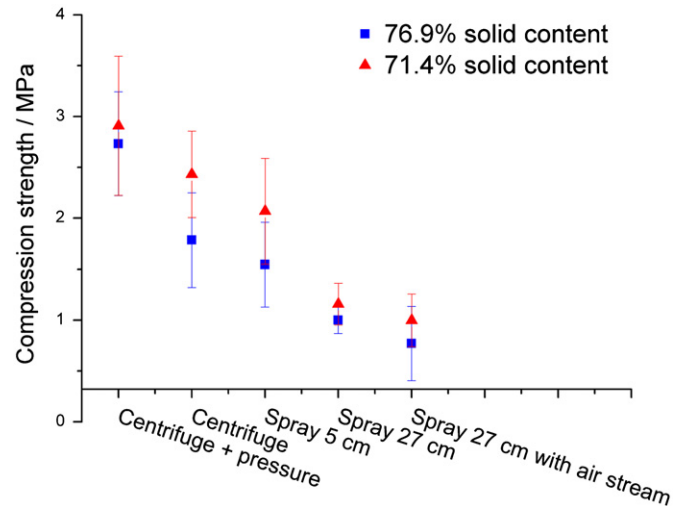


Fig. 12. Dependence of the compression strength on the different coating methods and solid contents for the second coating step.

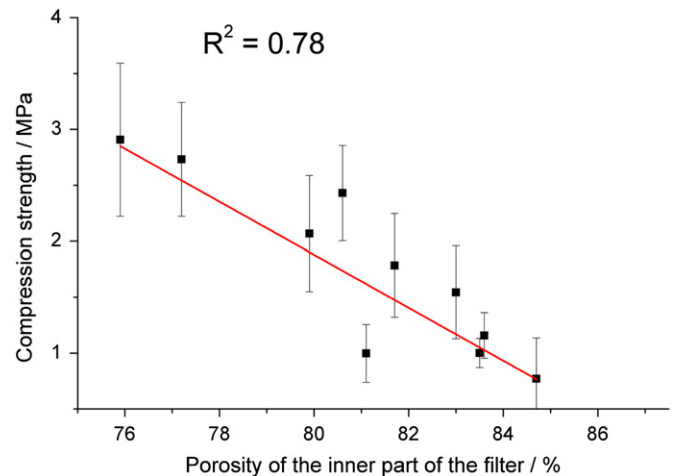


Fig. 13. Correlation between porosity of the inner part of the prepared filters and the mean compression strength.

mechanical strength, although the one with the higher viscosity has the lower values; but the differences are within the standard deviation. The higher strength of the 5 cm sprayed samples is in accordance to the CT-results. The centrifuged filters achieved the best mechanical properties. The reason for the improvement of the compression strength between the filters prepared with and without pressure is correlated to the slightly higher mass (see Table 2) and/or the use of the pressure while dipping into the slurry. In sum up there is a good correlation between the porosity distribution and the compression strength, (Fig. 13).

A Small-Impingement test was carried out with two filter of each variation. All the filters pass the test.

4. Conclusion

The “replica process” was used to prepare open ceramic porous filters based on alumina. The influence of different

processing parameters were investigated and correlated to the structure and to the mechanical properties.

The variations of the slurry additives for the first coating showed that also small changes in the amount of Axilat RH 50 MD have an influence on the required water amount and thereby affect the applied mass and the rheological behavior. The other used additives (in the chosen limits) haven't a large influence on the applied mass or the rheological behavior.

The used method for the second coating has a large influence on the homogeneity and affects so the compression strength. Thereby it is essential to force the slurry into the middle of the foam with an additional applied pressure during the dipping into the slurry or to process with a short distance (spraying with distance 5 cm) while spraying. Based on CT-results for centrifuging a low viscous fluid (71.4 wt% solid content) slurry would be an advantage. For the spraying it seems that the slurry with the higher viscosity (76.9 wt% solid content) is the better choice.

Acknowledgments

The authors would like to thank the German Research Foundation (DFG) for supporting these investigations in terms of the Collaborative Research Center 920 "Multi-Functional Filters for Metal Melt Filtration—a contributions towards Zero Defect Materials", Subproject A02 and S03. The authors also would like to acknowledge the support of K. Moritz.

References

- [1] B. Prillhofer, H. Antrekowitsch, Abscheidung von nichtmetallischen Einflüssen bei der Raffination von Aluminiumlegierungen, *BHM* 152 (3) (2007) 53–61.
- [2] K. Schwartzwalder, H. Somers, A.V. Somers, Method of Making Porous Ceramic Articles, Patent US 3,090,094, 1963.
- [3] X. Pu, F. Qui, L. Huang, Novel method to optimize the structure of reticulated porous ceramics, *Journal of the American Ceramic Society* 87 (7) (2004) 1392–1394.
- [4] M. Hasterok, C. Wenzel, C.G. Aneziris, Processing of ceramic preforms for TRIP-matrix-composites, *Steel Research International* 82 (9) (2011) 1032–1039.
- [5] C.G. Anezires, A. Ansorge, H. Jaunich, New approaches of carbon bonded foam filters for filtration of large castings, *cfi-Berichte der DKG* 85 (10) (2008) E44–E47.
- [6] X. Yao, S. Tan, Z. Huang, Effect of recoating slurry viscosity on the properties of reticulated porous silicon carbide ceramics, *Ceramics International* 32 (2006) 137–142.
- [7] A.R. Studart, U.T. Gonzenbach, E. Tervoort, Processing routes to macroporous ceramics: a review, *Journal of the American Ceramic Society* 89 (6) (2006) 1771–1789.
- [8] M. Montanaro, Y. Jorand, G. Fantozzi, A. Negro, Ceramic foams by powder processing, *Journal of the European Ceramic Society* 18 (1998) 1339–1350.
- [9] M. Dressel, S. Reinsch, R. Schadrak, S. Benemann, Burnout behavior of ceramic open cell polyurethane (PU) sponges, *Journal of the European Ceramic Society* 29 (2009) 3333–3339.
- [11] C. Lautensack, M. Giertzsch, M. Godehardr, K. Schladitz, Modeling a ceramic foam using locally adaptable morphology, *Journal of Microscopy* 230 (3) (2008) 396–404.